The Wood equation allows consistent fitting of individual antibody-response profiles of Zika virus or SARS-CoV-2 infected patients

J Denis, A Garnier, D Claverie, F de Laval, S Attoumani, B Tenebray, G A Durand, B Coutard, I Leparc-Goffart, Jean-Nicolas Tournier, et al.

Heliyon 9 (2023) e21945

Contents lists available at ScienceDirect

Heliyon

journal homepage: www.cell.com/heliyon

The Wood equation allows consistent fitting of individual antibody-response profiles of Zika virus or SARS-CoV-2 infected patients

J. Denis [a,b], A. Garnier [a], D. Claverie [c], F. De Laval [d,e], S. Attoumani [f], B. Tenebray [b,f], G.A. Durand [b,f], B. Coutard [f], I. Leparc-Goffart [b,f], J.N. Tournier [a,g,h], S. Briolant [i,j], C. Badaut [f,k,*]

[a] Unité Interaction Hôte - Pathogene, Institut de Recherche Biomédicale des Armées, Brétigny-sur-Orge, France
[b] Centre National de Référence des Arbovirus, Institut de Recherche Biomédicale des Armées, Marseille, France
[c] Unité de Neurophysiologie du Stress, Institut de Recherche Biomédicale des Armées, 1 place du Général Valérie André BP73, Brétigny-sur-Orge Cedex, France
[d] Service de Santé des Armées, Centre d'Epidémiologie et de Santé Public des Armées, Marseille, France
[e] Aix Marseille Université, INSERM, SESSTIM, Science Economique & Sociales de la Santé & Traitement de l'Information Médicale, Marseille, France
[f] Unité des Virus Émergents (UVE: Aix-Marseille Univ - IRD 190 - Inserm 1207 - IHU Méditerranée Infection), Marseille, France
[g] Institut Pasteur, Innovative Vaccine Laboratory, Paris, France
[h] Ecole du Val-de-Grâce, Paris, France
[i] Unité de Parasitologie et Entomologie, Département de Microbiologie et des Maladies Infectieuses, Institut de Recherche Biomédicale des Armées, Marseille, France
[j] Aix Marseille Université, IRD, AP-HM, SSA, UMR vecteurs – Infections Tropicales et Méditerranéennes (VITROME), IHU – Méditerranée Infection, Marseille, France
[k] Unité de virologie, Institut de Recherche Biomédicale des Armées, Brétigny-sur-Orge, France

ARTICLE INFO

Keywords:
Humoral immune response
Curve fit
Zika virus
SARS-CoV-2
Kinetic
Wood equation

ABSTRACT

Antibody kinetic curves obtained during a viral infection are often fitted using aggregated patient data, hiding the heterogeneity of individual humoral immune responses. Individual antibody responses can be modeled using the Wood equation and grouped according to their profile. Such modeling takes into account several important kinetic parameters, such as the day when antibody detection becomes positive [daypos], the day of the maximal response [daymax], the maximum antibody level [levelmax], and the day when antibody detection becomes negative [dayneg]. Potential associations between these profiles and studied factors can then be tested.

1. Introduction

Infectious diseases induce an innate immune response, followed by adaptative cellular and humoral immune responses, the humoral response generally leading to increased antibody (Ab) levels (IgM and IgG in the blood compartment). Interestingly, several studies have shown a difference in the kinetic profiles of anti-Zika virus (ZIKV) Abs depending on a previous dengue infection [1]. Disease severity following infection with severe acute respiratory syndrome coronavirus 2 (SARS-CoV-2) has also been shown to be

* Corresponding author. Unité de virologie, Institut de Recherche Biomédicale des Armées, Brétigny-sur-Orge, France
E-mail address: cbadaut@gmail.com (C. Badaut).

https://doi.org/10.1016/j.heliyon.2023.e21945
Received 22 December 2021; Received in revised form 27 October 2023; Accepted 31 October 2023
Available online 7 November 2023

Table 1
Characteristics of the patients and their humoral immune response calculated using Wood parameters.

Patient	Age	Sex	Imm. scar	Antibody type	ELISA target	a	b	c	d	r^2	Day pos	Day max	Level max	Day neg
P1	26	F	ND	IgG	RBD SARS-CoV-2	1.513	0.87006	0.015995	1	0.86	0	54	20.5	377
P2	51	M	ND	IgG	RBD SARS-CoV-2	0.33971	1.4658	0.034283	1	0.77	2	43	19.3	251
P3	39	M	No	IgM	ZIKV	0.1585	1.8327	0.094116	1	0.94	6	19	5.9	49
P3	39	M	No	IgG	ZEDIII	0.017577	1.4083	0.0092013	1	0.97	3	153	5.1	680
P4	41	M	Yes	IgM	ZIKV	0.39849	1.2568	0.08709	1	0.92	6	14	3.2	32
P4	41	M	Yes	IgG	ZEDIII	0.10658	1.2549	0.006617	1	0.86	4	190	21.9	1660
P5	42	M	ND	IgG	ZEDIII	0.12655	0.7574	0.005674	1	0.83	8	133	2.4	598
Pooled data	None	None	None	IgG	None	0.0505062	1.2854	0.0075445	1	0.31	4	170	10.3	832

Patients P1 and P2 were infected by SARS-CoV-2 and patients P3, P4, and P5 by ZIKV.
Imm. scar: immunological scar, a, b, c, d: Wood parameters, r^2: reliability factor, Day_{pos}: day when antibody detection becomes positive, Day_{max}: day of maximal response, $Level_{max}$: maximal level of antibody, Day_{neg}: day when the antibody detection becomes negative, ND: not documented, F: female, M: male. RBD SARS-CoV-2: receptor-binding domain of severe acute respiratory syndrome coronavirus 2, ZIKV: Zika virus, ZEDIII: recombinant domain III of the ZIKV envelope protein.

related to the associated Ab kinetics [2].

The humoral immune response is characterized by the level of the Ab response and the day of their first detection, maximal concentration, and disappearance. In many studies in which antibody production is followed after vaccination, the characteristic

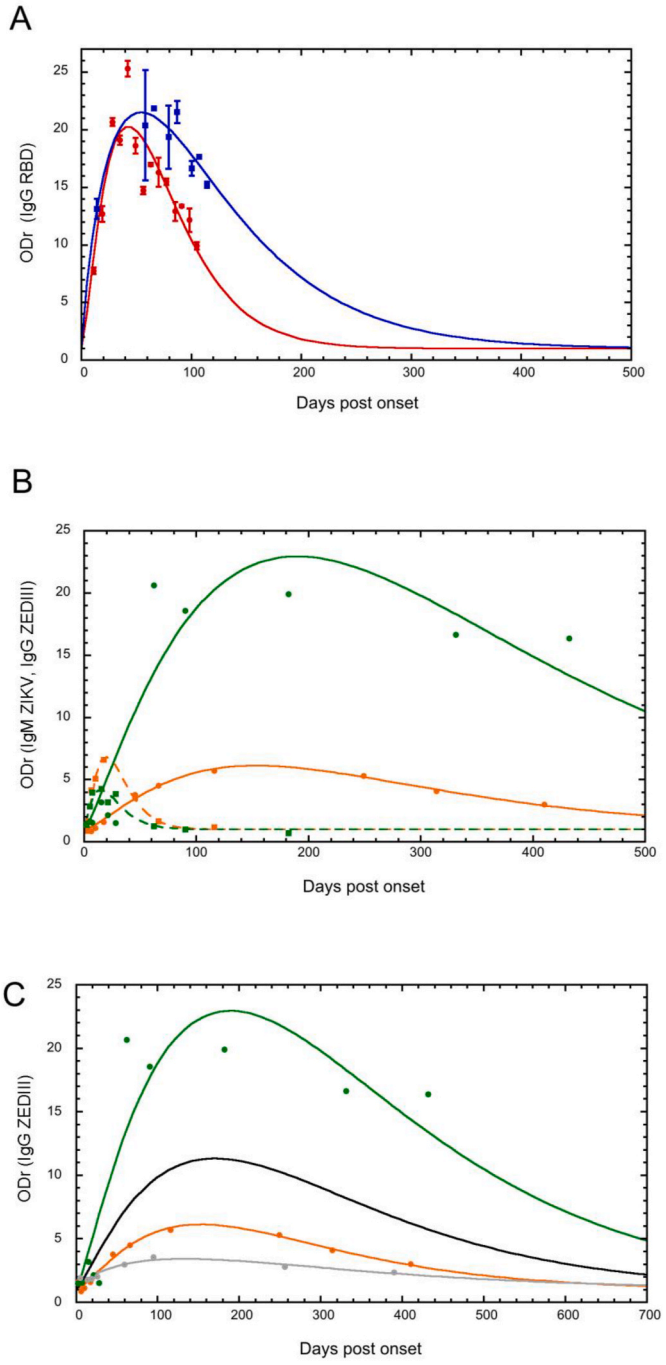

Fig. 1. Modeling of antibody kinetics after ZIKV infection **(A)** IgG levels of two SARS-CoV-2-infected patients, P1 (blue) and P2 (red), and **(B)** IgM (squares, dotted line) and IgG (circles, solid line) levels of ZIKV-infected patients, P3 (orange) and P4 (green), were fitted using the Wood equation. **(C)** The data from three patients were plotted and the curve fit performed using the Wood equation for each patient (P3: orange, P4: green, P5: grey). The black curve is the fitted curve using pooled data of the three patients P1, P2, and P3. The IgM curve reliability factor r is 0.97 and 0.96 for P3 and P4, respectively, and those of the IgG curve 0.93, 0.88, 0.99, 0.92, 0.91, and 0.56 for P1, P2, P3, P4, P5, and the black curve, respectively. The means and standard deviations of the optical density ratios are presented in panel A. (For interpretation of the references to colour in this figure legend, the reader is referred to the Web version of this article.)

constants of the Ab response are calculated using the equation obtained by fitting the often incomplete data of all patients [3,4]. However, using aggregated data to obtain an average kinetic curve does not take into account the heterogeneity of the individual humoral immune responses.

Most linear mixed models already developed to follow the dynamics of the Ab response focus solely on the decline in Ab concentration, long after the peak, in the context of post-vaccination [5–7], without taking into account the beginning of the Ab response. Other mathematical models have also been used to describe the complete dynamics of Ab responses following anti-hepatitis A [8] or anti-Ebola virus [9] vaccination. They are based on ordinary differential equations requiring the hypothesis that antibodies are produced by both short- and long-lived blood cells. In these models, immune memory is not considered, which is a limitation, in particular in terms of predicting the response to exposure to wildtype virus. Moreover, the samples fitted in these studies, of which only a few were from around Daymax, did not allow precise determination of the day when the maximum antibody level was reached.

However, all these parameters can be extracted following modeling of the Ab response using Wood's equation ($yn = a\ nb\ exp(-cn)$). This equation was first routinely used to follow milk production by cattle [10], a biological process of protein production. It is now commonly used to adjust the kinetics of viraemia [11] and estimate IgG concentrations after vaccination [12]. In contrast to other models, The Wood equation does not require any conditions of application nor biological hypotheses. Here, we used this equation to model the individual Ab responses of patients, whose samples were collected over several weeks, to obtain the kinetic parameters of

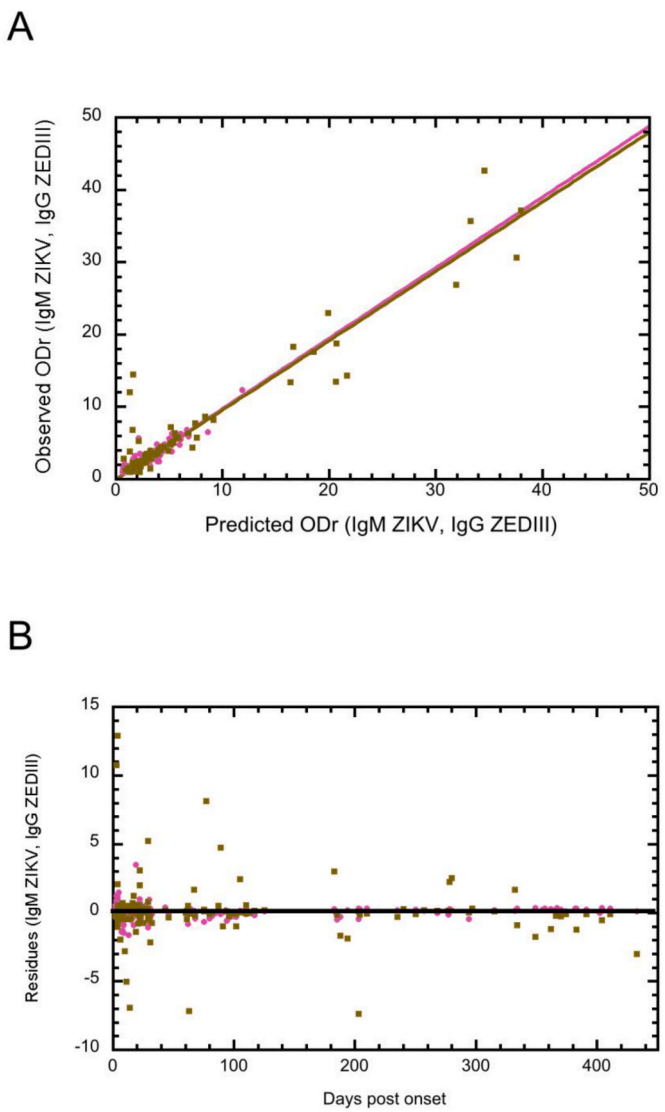

Fig. 2. Goodness of fit of the Wood equation **(A)** The modeled values corresponding to each observed ODr were calculated for each patient using the a, b, c, and d paremetters, for anti-ZIKV IgM (purple squares) and anti-ZEDIII IgG (brown squares) and were plotted ($n_{(IgM\ ZIKV)} = 171$, $n_{(IgG\ ZEDIII)} = 163$). The fit of the linear regression was $r^2 = 0.89$ for anti-ZIKV IgM and 0.90 for anti-ZEDIII IgG.**(B)** The residuals were calculated and are presented. (For interpretation of the references to colour in this figure legend, the reader is referred to the Web version of this article.)

their Ab responses and to compare this approach to that using aggregated data. We show that this equation allows modeling of the total kinetics of the Ab response, as well as extrapolation of unavailable constants (the day when antibody detection becomes positive [daypos], the day of the maximal response [daymax], the maximum level of antibody [levelmax], and the day when antibody detection becomes negative [dayneg]) as characteristics of the system studied. We thus selected two natural viral infections with different modes of transmission and clinical manifestation: i) Zika virus (ZIKV) and ii) SARS-CoV-2. To evaluate this mathematical model, we followed the levels of IgM against the entire Zika virus and those of IgG against ZEDIII, which are both virus specific [13]. For the first time, the follow up of ZIKV-infected patients allowed determination of the reliability of a mathematical model.

2. Materials and methods

Ethical approval was given by the Comité de Protection des Personnes Sud Méditerranée I for the "Etude descriptive prospective de la maladie à virus Zika au sein de la communauté de défense des Forces Armées en Guyane ZIFAG" and was registered on February 29, 2016 as RCB: 2016-A00394-47. All necessary patient/participant consent was obtained and the appropriate institutional forms archived.

Serial serum samples were obtained from 19 ZIKV-infected patients included in a previously published cohort survey [14] and two SARS-CoV-2-infected patients from another study [15]. The two SARS-CoV-2-infected patients, who had mild or moderate disease, were called P1 and P2, respectively.

An ELISA using total inactivated ZIKV and recombinant domain III of the ZIKV envelope protein (ZEDIII) was used to determine IgM and IgG levels, respectively [13]. Anti-SARS-CoV-2 IgG levels were determined using the receptor-binding domain (RBD) of the spike envelope glycoprotein as the target [16]. Optical-density ratios (ODrs) were calculated by dividing the OD obtained with the target for the same sera with the blank. The antibody levels following infection with ZIKV or SARS-CoV-2 were fitted using the Wood model ($ODr = a.Day^{b}.exp^{(-c.Day)} + d$; where a, b, and c are the individual parameters of the Wood function [10] and d is the residual ODr obtained at infinite time, considering that the minimum Y of an ODr is approximately 1) and KaleidaGraph 4.5 software. The positive threshold of the ODr was calculated as the mean + 3 standard deviations for each studied antibody and antigenic target (IgM for ZIKV = 3.00, IgG for EDIII = 1.54, IgG for RBD = 2.40) [13]. Day_{max} was calculated following the formula: $day_{max} = b/c$. The maximum IgG levels ($level_{max}$) were calculated following the formula: $level_{max} = a(b/c)^{b}exp^{(-b)}$ [11]. The Wood curve was plotted day by day for each condition. Both day_{pos} and day_{neg} were interpolated from each curve. The results obtained with the data of each patient were compared to the mean of day_{max} and $level_{max}$ for all patients combined. The correlation between quantitative variables was tested using Spearman's correlation test. P-values <0.05 were considered significant.

3. Results

The antibody kinetic profile parameters from five patients (two infected by SARS-CoV-2 and three by ZIKV) are presented in Table 1. For P1, the value for day_{pos} was 0, day_{max} 54, IgG $level_{max}$ 20.5, and day_{neg} 377 and for P2 the values were day_{pos} 2, day_{max} 43, IgG $level_{max}$ 19.3, and day_{neg} 251 for SARS-CoV-2 (Fig. 1A). For P3, who presented no immunological scar, the value for day_{pos} was 6, day_{max} 19, $level_{max}$ 5.9, and day_{neg} 49 for IgM and the corresponding values for IgG were day_{pos} 3, day_{max} 154, $level_{max}$ 5.1, and day_{neg} 680. The corresponding values for P4 were day_{pos} 6, day_{max} 14, $level_{max}$ 3.2, and day_{neg} 32 for IgM and day_{pos} 4, day_{max} 190, $level_{max}$

Table 2
Characteristics of anti-ZEDIII IgG kinetics of 19 Zika virus-infected patients.

Patient	Age	Sex	Imm scar	a	b	c	d	r^2	Day max	Level max
Z001	31	M	No	0.092566	0.97392	0.011703	1	0.78	83	2.6
Z002	53	F	No	0.0099388	1.6195	0.012829	1	0.99	126	5.0
Z003	42	M	No	0.091431	1.7582	0.11474	1	0.63	15	1.9
Z006	45	M	ND	1.4519	0.52678	0.0082031	1	0.64	64	7.7
Z007	59	F	Yes	5.0932	0.74602	0.01479	1	0.72	50	45.0
Z011	37	M	No	0.061804	1.1204	0.015594	1	0.86	72	2.4
Z013	31	F	Yes	0.22282	0.86004	0.011256	1	0.82	76	3.9
Z016	42	M	No	0.081397	0.88882	0.0079857	1	0.91	111	2.2
Z018	41	F	Yes	0.0024708	2.2639	0.033662	1	0.98	67	3.5
Z019	34	F	No	0.0018635	2.032	0.015418	1	0.94	132	5.0
Z020	42	M	No	0.00066167	2.3664	0.010669	1	0.98	222	22.2
Z021	29	M	No	0.12932	0.81286	0.010517	1	0.81	77	2.0
Z027	43	F	no	0.032182	1.6132	0.012727	1	0.93	127	15.8
Z030	39	M	No	0.01493	1.4459	0.0093553	1	0.97	155	5.1
Z032	42	M	Yes	0.11147	0.78885	0.0058377	1	0.84	135	2.4
Z038	46	M	Yes	0.6422	0.80863	0.020974	1	0.59	39	5.5
Z039	41	M	Yes	0.092568	1.2859	0.0067244	1	0.85	191	22.0
Z045	32	F	No	0.10269	0.83414	0.0089983	1	0.93	93	2.0
Z046	35	M	Yes	0.13936	0.8489	0.0072951	1	0.93	116	3.4

Imm. scar: immunological scar, a, b, c, d: Wood parameters, r^2: reliability factor, Day_{pos}: day when antibody detection to ZEDIII becomes positive, Day_{max}: day of maximal response, $Level_{max}$: maximal level of antibody, Day_{neg}: day when the antibody detection becomes negative, ND: not documented, F: female, M: male.

21.9, and day_{neg} 1660 for IgG (Fig. 1B). Finally, for patient P5, the values for IgG were day_{pos} 8, day_{max} 133, $level_{max}$ 2.4, and day_{neg} 598. The extrapolation of day_{max} (170 days) and day_{neg} (832 days) obtained with the curve fit of the pooled data of P3, P4, and P5 (pooled data) was different from the calculated mean of day_{max} (159 days) and day_{neg} (979 days) of the three individual curves (Fig. 1C). The correlations were high ($r^2 \geq 0.83$), except for the pooled data curve ($r^2 = 0.31$) (Table 1).

We evaluated the goodness of fit of the Wood equation. The modeled ODr was obtained for each patient using their Wood parameters. The observed and modeled ODr (Fig. 2A) of IgM ZIKV and IgG ZEDIII were compared. The linear regression showed a very good fit, with a $r^2 = 0.94$, ($n = 334$ ($n_{(IgM\ ZIKV)}$ 171, $n_{(IgG\ ZEDIII)} = 163$)). The residuals were also calculated and are presented in Fig. 2B.

In addition, we performed the same analyses as those performed on three patients using a larger sample of ZIKV-infected patients ($n = 19$) to obtain a statistical view. All patient characteristics are described in Table 2. Day_{max} and $level_{max}$ were plotted for each patient (Fig. 3A, red circles). The means of these values (green square, $day_{max} = 97$; $level_{max} = 7.9$) were compared to those of day_{max} (147) and $level_{max}$ (6) (blue square) of the curve obtained by fitting the aggregated data (Fig. 3B).

4. Discussion

ODr values correlate with the concentrations and avidities of Abs, reflecting their affinity constants and, therefore, their ability to specifically bind to their target at a determined concentration, as we previously showed in Denis et al. [13]. Although ODrs are only semi-quantitative, the maximum ODrs and determined positivity thresholds are intrinsic values of the system and provide relevant relative values.

Many samples were missing for the first weeks after the infection of P1 with SARS-CoV-2, but adjustment of the obtained curve yielded results close to those of the adjusted curve for P2 (with a high reliability factor, $r2 \geq 0.77$). Samples are rarely taken on daypos

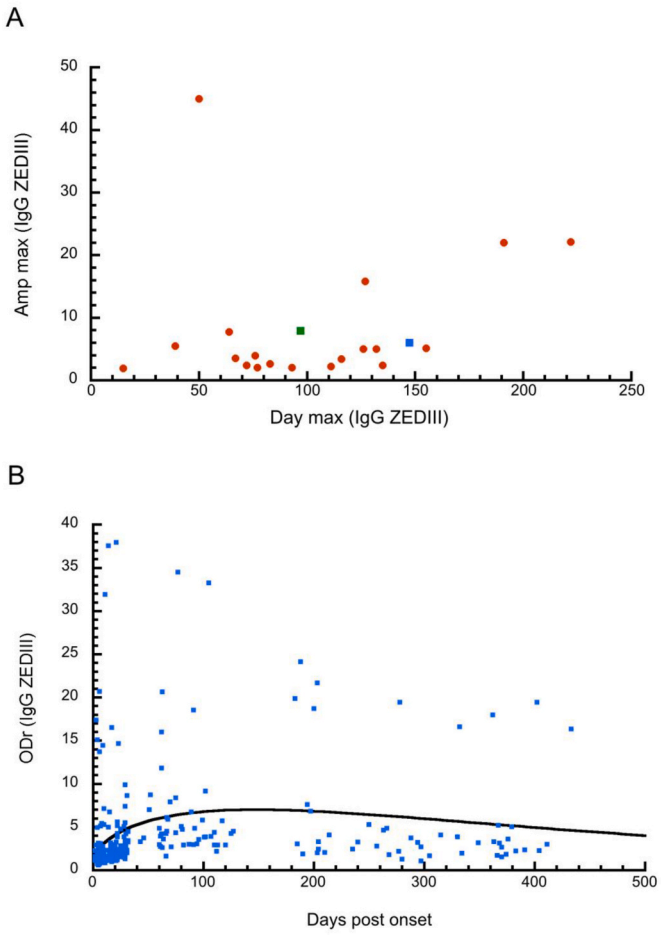

Fig. 3. Difference between Day_{max} of the mean curve and the mean Day_{max} of the individuals. **(A)** Day_{max} and $level_{max}$ of the individual antibody responses for ZIKV-infected patients ($n = 19$) were plotted (red circle). The mean of these values (green squares) and day_{max} and $level_{max}$ values of the curve obtained using aggregated data (blue squares) are different. **(B)** Day_{max} and $level_{max}$ were determined from the curve fit obtained from the aggregated data of the same 19 patients fitted with the Wood equation. (For interpretation of the references to colour in this figure legend, the reader is referred to the Web version of this article.)

or daymax and that for dayneg is often too late to be taken, sometimes hundreds of days after the onset of symptoms. However, these missing values can be extrapolated with high reliability (r2 close to 1). The Wood model fitted the data perfectly (Fig. 2), with a good r^2-value, using the higher number of samples obtained during the follow-up of these two patients. In most studies, the characteristic constants of the Ab response were calculated using the equation by fitting all of the (often incomplete) patient data [3,4].

In our study, the means of daymax and dayneg obtained from the curve fit of each patient ($r2 \geq 0.83$) were very different from those obtained from a single curve fit ($r2 = 0.31$) of the pooled data (Fig.s. 1C and 2B, respectively). The results obtained by fitting the aggregated data were highly different from those obtained by calculating the mean values of the individual data: daymax 147 and levelmax 6 for the aggregated data versus daymax 97 and levelmax 7.9 for the individual data. This leads to the loss of information and the ability to observe distinct populations and, finally, to a bias in the estimation of the kinetic parameters, as the immune response varies between patients, here, according to the immune status of the scar vis-à-vis the flavivirus.

The goodness of fit with the Wood equation was determined for both anti-ZIKV IgM and anti-ZEDIII IgG. Linear regression was performed and the result was exactly the same for both antibodies: the global reliability factor ($r2 = 0.94$) was identical and very good for both antibody kinetic profiles ($r^2 = 0.89$ for anti-ZIKV IgM and 0.90 for anti-ZEDIII IgG).

We applied this method to the humoral immune response directed against two viruses that have different modes of transmission and clinical manifestations. This method could allow patients to be linked to a past event, visible, for example, by the presence of a flavivirus immune scar or, more generally, host genetic diversity, specific strain fitness, or other observed phenotypes. The patient who was previously infected with a flavivirus had a lower level of IgM directed against ZIKV and a higher level of IgG than the patient without a serological scar directed against a flavivirus, as observed in a previous study [17].

Taking into consideration all the aggregated values from the patients, the average curve calculated from these data and the determination of daymax and levelmax could result in a distorted outcome because the curve profile may be biased if the data for a patient or group of patients within the aggregated data have an overrepresented number of points. It is therefore essential to generate an adjustment curve for each patient and to calculate the average daymax and levelmax from the results obtained with the individual curves. Generating an adjustment curve is roughly equivalent to normalizing the number of points for each patient. In addition, the comparison of each daymax and levelmax between patients can highlight patients or groups of patients who are outliers, for whom other characteristics can be used to statistically group them.

This method, however, has several limitations. i) It depends on the targeted antigen used in the ELISA (the Wood values, such as daymax and levelmax, may vary). Thus, the involvement of the protein or domain targeted in various mechanisms, such as antigens for immune escape or cell receptor recognition, could be highlighted. ii) It depends on the hypothesized mechanism. The antigen must be chosen considering the mechanism involved in the disease. Thus, the ZEDIII and RBD proteins were selected because of their involvement in viral entry into cells. Both are targets of neutralization antibodies. Finally, the protein target must participate in the process involved in the appraised phenotype. iii) Wood's equation can only perfectly model an Ab kinetic response when at least two points are present in the increasing phase of the curve and three in the decreasing phase. This study thus represents a proof of concept of the possible use of this equation in the context of Zika infection. We highlight the importance of considering the Ab kinetic response individually. Indeed, mathematically, the mean of each antibody response was different from the global mean of the aggregated antibody responses. Nevertheless, we did not search for differences that characterized different clusters of responses in this study due to the low number of patients. This aspect will be investigated in a future application of this preliminary study.

In conclusion, application of the Wood model to individual Ab responses, instead of aggregated Ab responses, could make it possible to consider individual Ab response profiles, opening the door to personalized medicine. The identification and clustering of statistically different kinetic profiles for patients would make it possible to compare various characteristics, such as age, sex, or genotype, within each group and to relate a typical profile group, for example, to the seriousness of observed clinical signs or other observed phenotypes. The ability to extrapolate the daymax and levelmax from the curve is an important achievement, as this information could have implications for disease prognosis and therapy, such as for SARS COV2 [18]. This could subsequently be useful for predicting an association, for example, with the intensity or evolution of the pathology (as observed, for example, by Sejdeic et al. [19]) and perhaps even in demonstrating, a posteriori, the association of a type of humoral immune response to the improvement or worsening of a patient's condition. Such identification could contribute to the exploration of the mechanisms involved in severe forms and solutions for treating patients with a similar kinetic profile. The Wood curve could also be helpful in determining the diagnostic window and would be useful for the diagnosis of diseases such as dengue-like syndrome or Covid-19.

5. Funding information

This work was partially supported by the European Union's Horizon H2020 Project "Advanced Nanosensing platforms for Point of care global diagnostics and surveillance" (CONVAT) (No 101003544) and partially funded by the Direction Générale de l'Armement and the Service de Santé des Armées (Biomedef PDH-2-NRBC-2-B-2111), and the Direction centrale du Service de santé des armées (grant IDs: 2016RC10).

Data availability statement

Data associated with our study have not been deposited into a publicly available repository. The raw data that support the finding of this study are available from the corresponding author.

Additional information

The clinical trial described in this paper was registered at Comite de Protection des Personnes Sud Mediterranee I, RCB: 2016-A00394-47.

CRediT authorship contribution statement

J. Denis: Conceptualization, Data curation, Formal analysis, Methodology, Validation, Visualization, Writing – original draft. **A. Garnier:** Data curation, Methodology, Validation. **D. Claverie:** Conceptualization, Data curation, Formal analysis, Investigation, Methodology, Validation, Writing – original draft. **F. De Laval:** Conceptualization, Formal analysis, Methodology, Resources, Project administration. **S. Attoumani:** Conceptualization, Data curation, Investigation, Methodology, Resources. **B. Tenebray:** Conceptualization, Data curation, Methodology, Resources. **G.A. Durand:** Methodology, Resources, Supervision, Validation, Writing – review & editing. **B. Coutard:** Investigation, Resources, Supervision, Validation. **I. Leparc-Goffart:** Methodology, Project administration, Resources, Supervision. **J.N. Tournier:** Conceptualization, Methodology, Validation, Writing – review & editing. **S. Briolant:** Methodology, Project administration, Supervision, Validation, Writing – original draft, Funding acquisition. **C. Badaut:** Conceptualization, Funding acquisition, Investigation, Methodology, Project administration, Supervision, Validation, Visualization, Writing – original draft.

Declaration of competing interest

The authors declare that they have no known competing financial interests or personal relationships that could have appeared to influence the work reported in this paper.

Aknowlegment

The authors would like to thank Ombeline Lamer for fruitful discussions.

References

[1] L. Barzon, E. Percivalle, M. Pacenti, F. Rovida, M. Zavattoni, P. Del Bravo, A.M. Cattelan, G. Palù, F. Baldanti, Virus and antibody dynamics in travelers with acute Zika virus infection, Clin. Infect. Dis. 66 (8) (2018) 1173–1180.

[2] N.M.A. Okba, M.A. Müller, W. Li, C. Wang, C.H. GeurtsvanKessel, V.M. Corman, et al., Severe acute respiratory syndrome coronavirus 2-specific antibody responses in coronavirus disease patients, Epub 2020/04/09, Emerg. Infect. Dis. 26 (7) (2020) 1478–1488, https://doi.org/10.3201/eid2607.200841. PubMed PMID: 32267220; PubMed Central PMCID: PMCPMC7323511.

[3] F.A. Bozza, A. Moreira-Soto, A. Rockstroh, C. Fischer, A.D. Nascimento, A.S. Calheiros, et al., Differential shedding and antibody kinetics of Zika and chikungunya viruses, Brazil, Emerg. Infect. Dis. 25 (2) (2019) 311–315, https://doi.org/10.3201/eid2502.180166. PubMed PMID: 30666934; PubMed Central PMCID: PMC6346451.

[4] A. Padoan, L. Sciacovelli, D. Basso, D. Negrini, S. Zuin, C. Cosma, et al., IgA-Ab response to spike glycoprotein of SARS-CoV-2 in patients with COVID-19: a longitudinal study, Epub 2020/04/29, Clinica chimica acta; international journal of clinical chemistry 507 (2020) 164–166, https://doi.org/10.1016/j.cca.2020.04.026. PubMed PMID: 32343948; PubMed Central PMCID: PMCPmc7194886.

[5] F.E. Nommensen, S.T. Go, D.M. MacLaren, Half-life of HBs antibody after hepatitis B vaccination: an aid to timing of booster vaccination, Epub 1989/10/07, Lancet (London, England) 2 (8667) (1989) 847–849, https://doi.org/10.1016/s0140-6736(89)93009-2. PubMed PMID: 2571769.

[6] K. Desai, L. Coudeville, F. Bailleux, Modelling the long-term persistence of neutralizing antibody in adults after one dose of live attenuated Japanese encephalitis chimeric virus vaccine, Epub 2012/02/22, Vaccine 30 (15) (2012) 2510–2515, https://doi.org/10.1016/j.vaccine.2012.02.005. PubMed PMID: 22342547.

[7] B. Cheuvart, M. Burgess, F. Zepp, J. Mertsola, J. Wolter, L. Schuerman, Anti-diphtheria antibody seroprotection rates are similar 10 years after vaccination with dTpa or DTPa using a mathematical model, Epub 2004/11/09, Vaccine 23 (3) (2004) 336–342, https://doi.org/10.1016/j.vaccine.2004.06.012. PubMed PMID: 15530678.

[8] M. Andraud, O. Lejeune, J.Z. Musoro, B. Ogunjimi, P. Beutels, N. Hens, Living on three time scales: the dynamics of plasma cell and antibody populations illustrated for hepatitis a virus, Epub 2012/03/08, PLoS Comput. Biol. 8 (3) (2012), e1002418, https://doi.org/10.1371/journal.pcbi.1002418. PubMed PMID: 22396639; PubMed Central PMCID: PMCPMC3291529.

[9] C. Pasin, I. Balelli, T. Van Effelterre, V. Bockstal, L. Solforosi, M. Prague, et al., Dynamics of the humoral immune response to a prime-boost ebola vaccine: quantification and sources of variation, Epub 2019/06/28, J. Virol. 93 (18) (2019), https://doi.org/10.1128/jvi.00579-19. PubMed PMID: 31243126; PubMed Central PMCID: PMCPMC6714808.

[10] P.D.P. Wood, Algebraic model of the lactation curve in cattle, Nature 216 (5111) (1967) 164–165. PubMed PMID: WOOD1967.

[11] Z.U. Islam, S.C. Bishop, N.J. Savill, R.R. Rowland, J.K. Lunney, B. Trible, et al., Quantitative analysis of porcine reproductive and respiratory syndrome (PRRS) viremia profiles from experimental infection: a statistical modelling approach, PLoS One 8 (12) (2013), e83567, https://doi.org/10.1371/journal.pone.0083567. PubMed PMID: 24358295; PubMed Central PMCID: PMCPMC3866253 Canada.

[12] M. Andraud, C. Fablet, P. Renson, F. Eono, S. Mahé, O. Bourry, et al., Estimating parameters related to the lifespan of passively transferred and vaccine-induced porcine reproductive and respiratory syndrome virus type I antibodies by modeling field data, Epub 2018/02/13, Front. Vet. Sci. 5 (2018) 9, https://doi.org/10.3389/fvets.2018.00009. PubMed PMID: 29435455; PubMed Central PMCID: PMCPMC5796902.

[13] J. Denis, S. Attoumani, P. Gravier, B. Tenebray, A. Garnier, S. Briolant, et al., High specificity and sensitivity of Zika EDIII-based ELISA diagnosis highlighted by a large human reference panel, Epub 2019/09/21, PLoS Neglected Trop. Dis. 13 (9) (2019), e0007747, https://doi.org/10.1371/journal.pntd.0007747. PubMed PMID: 31539394; PubMed Central PMCID: PMCPMC6774568.

[14] F. de Laval, H. d'Aubigny, S. Mathéus, T. Labrousse, A.L. Ensargueix, E.M. Lorenzi, F.X. Le Flem, N. André, D. Belleoud, I. Leparc-Goffart, D. Rousset, F. Simon, S. Briolant, Evolution of symptoms and quality of life during Zika virus infection: a 1-year prospective cohort study, J. Clin. Virol. 109 (2018 Dec) 57–62, https://doi.org/10.1016/j.jcv.2018.09.015. Epub 2018 Sep 26. PMID: 30523784.

[15] E. Billon-Denis, A. Ferrier-Rembert, A. Garnier, L. Cheutin, C. Vigne, E. Tessier, et al., Differential serological and neutralizing antibody dynamics after an infection by a single SARS-CoV-2 strain, Epub 2021/01/03, Infection 49 (4) (2021) 781–783, https://doi.org/10.1007/s15010-020-01556-8. PubMed PMID: 33387262; PubMed Central PMCID: PMCPMC7776280.

[16] D. Stadlbauer, F. Amanat, V. Chromikova, K. Jiang, S. Strohmeier, G.A. Arunkumar, et al., SARS-CoV-2 seroconversion in humans: a detailed protocol for a serological assay, antigen production, and test setup, Curr Protoc Microbiol 57 (1) (2020), e100, https://doi.org/10.1002/cpmc.100. PubMed PMID: 32302069; PubMed Central PMCID: PMCPMC7235504.

[17] Cucunawangsih, N.P. Lugito, A. Kurniawan, Immunoglobulin G (IgG) to IgM ratio in secondary adult dengue infection using samples from early days of symptoms onset, Epub 2015/07/22, BMC Infect. Dis. 15 (2015) 276, https://doi.org/10.1186/s12879-015-1022-9. PubMed PMID: 26193930; PubMed Central PMCID: PMCPMC4509644.

[18] N.A. Osman, M.H. Hashish, W.M.K. Bakr, N.A. Osman, E.A. Omran, "Day 25": a temporal indicator of stabilization of mortality risk among COVID-19 patients with high viral load, Trop. Med. Health 50 (1) (2022) 92, https://doi.org/10.1186/s41182-022-00483-8. PMID: 36494866; PMCID: PMC9732988.

[19] A. Sejdic, A. Frische, C.S. Jørgensen, L.D. Rasmussen, R. Trebbien, A. Dungu, et al., High titers of neutralizing SARS-CoV-2 antibodies six months after symptom onset are associated with increased severity in COVID-19 hospitalized patients, Epub 2023/01/26, Virol. J. 20 (1) (2023) 14, https://doi.org/10.1186/s12985-023-01974-8. PubMed PMID: 36698135; PubMed Central PMCID: PMCPMC9875770.